Inorganic Chemistry

Article

pubs.acs.org/IC

Coordination of Terpyridine to Li^+ in Two Different Ionic Liquids

Klaus Pokorny,[†] Matthias Schmeisser,[†] Frank Hampel,[‡] Achim Zahl,[†] Ralph Puchta,[†] and Rudi van Eldik*,[†]

[†]Inorganic Chemistry, Department of Chemistry and Pharmacy, University of Erlangen—Nürnberg, Egerlandstrasse 1, 91058 Erlangen, Germany

[‡]Organic Chemistry, Department of Chemistry and Pharmacy, University of Erlangen—Nürnberg, Henkestrasse 42, 91054 Erlangen, Germany

Supporting Information

ABSTRACT: On the basis of ^7Li NMR experiments, the complex-formation reaction between Li^+ and the tridentate N-donor ligand terpyridine was studied in the ionic liquids $[emim][NTf_2]$ and $[emim][ClO_4]$ as solvents. For both ionic liquids, the NMR data implicate the formation of $[Li(terpy)_2]^+$. Density functional theory calculations show that partial coordination of terpyridine involving the coordination of a solvent anion can be excluded. In contrast to the studies in solution, X-ray diffraction measurements led to completely different results. In the case of $[emim][NTf_2]$, the polymeric lithium species $[Li(terpy)(NTf_2)]_n$ was found to control the stacking of this complex, whereas crystals grown from $[emim][ClO_4]$ exhibit the discrete dimeric species $[Li(terpy)(ClO_4)]_2$. However, both structures indicate that each lithium ion is formally coordinated by one terpy molecule and one solvent anion in the solid state, suggesting that charge neutralization and π stacking mainly control the crystallization process.

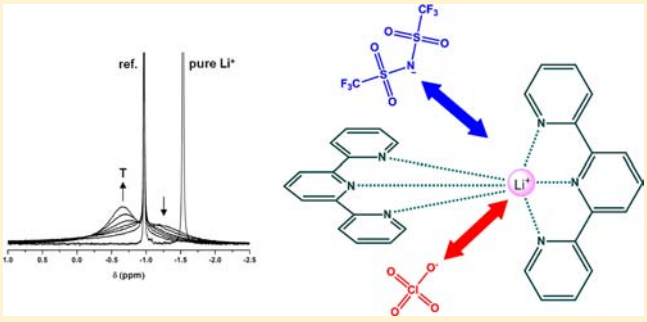

INTRODUCTION

Over the past decade, ionic liquids (ILs) have extensively been discussed as a promising class of new reaction media. The advantage of these "liquid salts" is based on the possibility to adjust their physicochemical properties such as density, melting point, polarity, or viscosity by the combination of a large variety of different possible cations and anions. It is thereby possible to systematically create series of IL solvents that are well-adapted to the requirements of a specific chemical reaction or process.[1,2] In this context, ILs are even denoted as "designer solvents" and have already been established in new technologies.[3]

Because ILs consist of cations and anions, they provide a completely different chemical environment for dissolved substrates as compared to conventional organic solvents or water. Consequently, this raises the question of how substrates are influenced by this unique environment (i.e., whether ILs do more than just serve as another solvent). Due to the large variety of properties and possible interactions, the subject "ionic liquids" turned out to be quite complex and has received widespread attention from scientists working on fundamental and applied aspects. Therefore, ILs and their behavior as solvents, reactants, catalysts, and cocatalysts are still not well understood, and many observations and effects cannot be sufficiently accounted for.

In terms of chemical reactions that involve dissolved metal compounds, such as in homogeneous catalysis, especially interactions between the anions of an IL and a catalytically active metal complex have to be considered, as most of the anions that form part of ionic liquids (e.g., Cl^-, CH_3COO^-, SCN^-, NO_3^- and $N(CN)_2^-$) can act as a Lewis base. As a consequence, the structure and reactivity of metal complexes can be seriously changed, either by occupying and blocking a vacant coordination site or by displacing weaker coordinated ligands.[4,5] Thus, detailed knowledge on the properties and reaction behavior of ILs is an important prerequisite to enable the efficient application of ILs in scientific research and technical processes.[6]

In this context, scientists have become more and more sensitive to the topic of donor and acceptor properties of ionic liquids and a growing number of publications attempt to generalize and categorize these properties to allow predictions on the behavior of ILs used as solvents.[7,8] However, it still remains difficult to make trustworthy predictions. Especially in the case of the nucleophilicity of ILs, or more precisely their anionic component, modifications within the first coordination sphere of a metal complex need not necessarily be an effect of a strong Lewis basicity, but can also originate from the very large excess of anions or their chemical hardness/softness compared to the dissolved substrate.

As shown by the work of Henderson[9] and Watanabe,[10] a detailed knowledge of the possible coordination behavior and

Received: August 12, 2013
Published: November 4, 2013

   dx.doi.org/10.1021/ic4020724 | Inorg. Chem. 2013, 52, 13167−13178

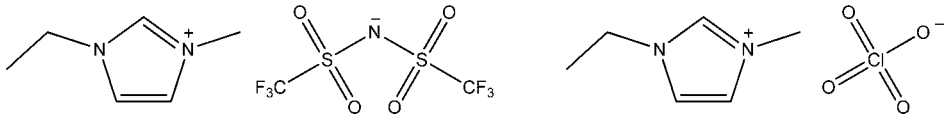

Figure 1. Schematic structures of the ionic liquids [emim][NTf_2] (left) and [emim][ClO_4] (right).

the nucleophilicity of anions is an essential prerequisite in the development of lithium batteries. Here, not only solid electrolytes[11] but also the combination of lithium salts and ILs has received growing interest. Therefore, studies on individual systems to understand and learn more about the various effects of ILs remain indispensable.

On the basis of our earlier work on the applicability of ILs as reaction media for processes in coordination chemistry[12−14] and the resulting interest in their donor and acceptor properties,[15] we now extended our earlier studies on the complexation of lithium ions by bidentate N-donor ligands[16] to study the influence of a tridentate N-donor ligand 2,2′:6′,2″-terpyridine (terpy) on the formation of such model compounds. To minimize solvent effects, we specially focused our attention on two ILs with low donor numbers and low coordination abilities.[15] We selected the ILs 1-ethyl-3-methylimidazolium bis(trifluoromethylsulfonyl)imide ([emim][NTf_2]),[17] a popular hydrophobic IL, and 1-ethyl-3-methylimidazolium perchlorate ([emim][ClO_4]), an uncommon IL that exhibits a hydrophilic character despite its low coordination ability (see Figure 1).[18,19] To follow the complex formation in solution, the chemical shift of the ^{7}Li NMR signal (abundance: 92.6%) was studied as a function of the added terpy concentration in reference to an external standard. Due to the fact that different equilibria between solvent molecules, ligands, and metal ions can generate structural motifs in solution that can differ from those derived from crystal structures, we also applied X-ray diffraction to gain more insight into the coordination pattern in the solid state. In addition, quantum chemical calculations (via density functional theory, DFT) were performed to obtain further support for the interpretation of the experimental results.

EXPERIMENTAL SECTION

Materials. All chemicals used in this study were of analytical reagent grade or of the highest purity commercially available. Terpyridine (2,6-bis(2-pyridyl)pyridine) and lithium perchlorate were purchased from Sigma Aldrich and used as received. Lithium ethylsulfate was obtained as a side product in the synthesis of the ionic liquid [emim][ClO_4] as described below. Lithium bis(trifluoromethylsulfonyl)imide and 1-ethyl-3-methylimidazolium bromide were obtained from Iolitec. 1-ethyl-3-methylimidazolium ethylsulfate was purchased from Solvent Innovation/Merck and purified as described below. All chemicals were stored under nitrogen atmosphere.

Synthesis of [emim][NTf_2]. To achieve a high purity IL, contaminants such as methylimidazole were removed by repeated crystallization of [emim]Br from a mixture of methanol and acetone. In this recrystallization procedure, [emim]Br was dissolved in an approximately 10% amount of methanol at 65 °C. After the mixtures cooled to room temperature, precooled acetone was added in a ratio of 1:1 compared to [emim]Br. Crystallization occurred overnight at a temperature of −23 °C. [emim][NTf_2] was then synthesized from [emim]Br and Li[NTf_2] by anion metathesis, as described elsewhere.[18] The water content was found to be 0.00% after the mixtures were dried under high vacuum for 5 days at 50 °C. Elemental analysis calculated (%) for $C_8H_{11}F_6N_3O_4S_2$: C, 24.55; H, 2.83; N, 10.74; S, 16.39. Found: C, 24.78; H, 2.65; N, 10.92; S, 16.54.

Purification of [emim][$EtSO_4$]. Traces of impurities were removed by repeated extraction with a mixture of dichloromethane and water in a volume ratio of 1:1. To achieve a higher optical purity, [emim][$EtSO_4$] was stirred for 1 week with activated charcoal (Acros Organics: Norit A SUPRA) under high vacuum at a temperature of 55 °C. After filtration, the water content was determined by Karl Fischer titration and found to be 0.03%. Elemental analysis calculated (%) for $C_8H_{16}N_2O_4S$: C, 40.66; H, 6.83; N, 11.86; S, 13.57. Found: C, 40.55; H, 6.66; N, 12.13; S, 13.24.

Synthesis of [emim][ClO_4]. The ionic liquid [emim][ClO_4] was prepared from $LiClO_4$ and [emim][$EtSO_4$] according to the direct anion metathesis procedure described elsewhere.[19] After the applied solvent mixture was removed and dried under high vacuum, [emim][ClO_4] was obtained as a colorless liquid in a yield of 94% with a water content of 0.02%. Elemental analysis calculated (%) for $C_6H_{11}ClN_2O_4$: C, 34.22; H, 5.26; N, 13.30. Found: C, 34.22; H, 5.50; N, 13.15. According to the requirements for an interim hazard classification (IHC), [emim][ClO_4] is not an explosive substance and passed the corresponding tests (UN 3a−UN 3d). However, care should be taken when working with [emim][ClO_4]. For further information read refs 19 and 20.

Synthesis of [Li(terpy)(NTf_2)]$_n$ (1). Solid terpy (210 mg; 0.9 mmol) was added under nitrogen atmosphere to a solution of Li[NTf_2] (86 mg; 0.3 mmol) in 3 mL of [emim][NTf_2]. The reaction mixture was heated to 75 °C under stirring to dissolve the solid terpy. Subsequently, the mixture was stored in the refrigerator at 3 °C. Within several days, colorless crystals appeared. Elemental analysis calculated (%) for $C_{17}H_{11}F_6LiN_4O_4S_2$: C, 39.24; H, 2.13; N, 10.77 S, 12.32. Found: C, 39.16; H, 2.05; N, 10.28; S, 12.20.

Synthesis of [Li(terpy)(ClO_4)]$_2$ (2). Solid terpy (210 mg; 0.9 mmol) was added to a solution of Li[ClO_4] (32 mg; 0.3 mmol) in 3 mL of [emim][ClO_4]. The reaction mixture was heated to 75 °C under stirring to dissolve the solid terpy. Subsequently, the mixture was stored in the refrigerator at 3 °C. Within several days, colorless crystals appeared. Elemental analysis calculated (%) for $C_{15}H_{11}ClLiN_3O_4$: C, 53.04; H, 3.26; N, 12.37. Found: C, 53.23; H, 3.41; N, 12.26.

Elemental Analysis. Elemental analyzers (Euro EA 3000 (Euro Vector) and EA 1108 (Carlo Erba)) were used for chemical analyses.

Karl Fischer Titrations. The water content of the ionic liquids was determined usinig a Coulomat C20 Karl Fischer titrator from Mettler-Toledo (Giessen, Germany).

NMR Studies. All operations were performed under nitrogen atmosphere by use of standard Schlenk techniques. In a typical series of measurements, a solution of terpyridine (0.25 M in the ionic liquid) was mixed in different volume ratios with a 0.05 M solution of the appropriate lithium salt. In each case, 530 μL of the lithium−ligand solution mixture was transferred under nitrogen atmosphere to a NMR tube and a glass capillary (i.d. = 1.16 mm) filled with an external standard (0.04 M $LiClO_4$ solution in DMSO-d_6) was placed inside the NMR tube. The ^{7}Li NMR spectra were recorded at a frequency of 155 MHz on a Bruker Avance DRX 400WB spectrometer equipped with a superconducting BC-94/89 magnet system. All measurements were performed at room temperature under ambient pressure.

X-ray Crystal Structure Determination. Suitable crystals of **1** and **2** were selected and mounted on loop on a SuperNova, Dual, Cu at zero, Atlas diffractometer. During data collection, the crystals were kept at 173.00(10) K. Using Olex2,[21] the structure was solved by direct methods with the SHELXS[22] structure solution program and refined with the SHELXL[22] refinement package applying least-squares minimization. CCDC-954464 and CCDC-954465 contain the supplementary crystallographic data on the structures of this publication. These data can be obtained free of charge from The

Cambridge Crystallographic Data Center via www.ccdc.cam.ac.uk/data_request/cif.

Quantum Chemical Calculations. All structures were fully optimized using the B3LYP hybrid density functional[23] and LANL2DZ[24] basis set augmented with polarization functions (further denoted as LANL2DZp).[25,26] All structures were characterized as minima by computation of vibration frequencies. The GAUSSIAN 03 suite of programs was used throughout.[27]

RESULTS AND DISCUSSION

^{7}Li NMR Studies. According to our earlier studies, ^{7}Li NMR measurements were used to determine the number of terpy molecules coordinated to the Li^+ ion in solution.[16] In a typical series of measurements, the concentration of the appropriate lithium salt was kept constant, while the concentration of the terpy ligand was varied up to a 9-fold excess of terpy over Li^+. The resulting chemical shift of the ^{7}Li signal was then plotted against the molar ratio of [terpy]:[Li^+]. When such a plot shows a clear discontinuity in the chemical shift, the appropriate [terpy]:[Li^+] ratio can be taken as the coordination number relative to the ligand.[28] Although such experiments can not reveal unequivocal information to which extent a remaining coordination site is indeed occupied by an anion of the employed ionic liquid, it can at least be estimated whether the first coordination sphere provides enough space for the coordination of solvent anions. With the assumption that a maximum of two terpy molecules can occupy the first coordination sphere of Li^+ (i.e., six coordination sites as indicated by DFT calculations (see below)), the number of remaining vacant coordination sites can be estimated from the determined coordination numbers.

Coordination of terpy to Li^+ in [emim][NTf_2]. Due to the sterical demanding and electron withdrawing trifluoromethyl groups, NTf_2^- based ILs exhibit a hydrophobic nature and a low coordinating ability. In addition, many of these liquid salts have low viscosities and high thermal as well as electrochemical stabilities.[18,29] Therefore, our investigations on the coordination of terpy to Li^+ were started using one of the most common ILs, [emim][NTf_2] (donor number (DN) = 11.2),[15] as solvent. To eliminate the possible disturbing influence of other anions, we in general used lithium salts that involve the same anion as compared to the employed ILs (i.e., in this case Li[NTf_2]).

Similar to our earlier observations on the coordination of bipyridine, the successive addition of terpy to Li^+ likewise resulted in a significant downfield shift of the ^{7}Li NMR signal up to a molar ratio of [terpy]:[Li^+] = 3:1, indicating a strong interaction between terpy and Li^+. On further addition of terpy, the ^{7}Li signal showed only a negligible drift and the first coordination sphere of Li^+ seemed to be saturated (see Figure 2).

Interestingly, at subequivalent concentrations of terpy, the ^{7}Li spectra exhibited significant line broadening. A closer look at these spectra clearly revealed a coalescence of various NMR signals. On the basis of the results of other groups, lithium ions dissolved in [emim][NTf_2] exhibit a solvent shell of two NTf_2^- anions.[30] These anions are coordinated as chelate ligands via the sulfonyl oxygen atoms and generate an overall tetrahedral coordination geometry at the Li^+ center. Thus, the coordination of terpy represents a successive displacement of a bidentate NTf_2^- ligand by a tridentate terpy ligand. As shown in Figure 3, the addition of only small amounts of terpy (0.1- up to 0.3-fold compared to Li^+) significantly affects the line shapes of the ^{7}Li

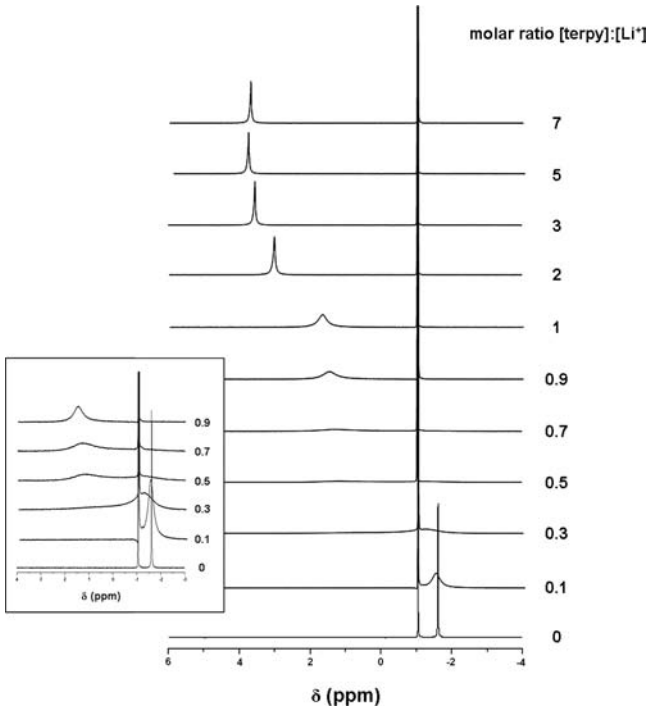

Figure 2. ^{7}Li NMR spectra recorded as a function of the molar ratio [terpy]:[Li^+] in [emim][NTf_2] at 25 °C. Inset: enlargement of the spectra at subequivalent addition of terpy.

signals, although the overall chemical shift remained small (less than 1 ppm). On varying the temperature (25−50 °C), the lines exhibited a distinct dynamic behavior. These observations can be attributed to weak interactions between terpy and Li^+, as well as the presence of dynamic equilibria between different lithium ligated species in the IL solution. Due to the large excess of Li^+ at these concentration levels and the high flexibility of terpy, the formation of different partially coordinated and/or bridged lithium species seems plausible and would best explain the small effect on the chemical shift. On increasing the concentration of terpy, the interaction between terpy and the individual lithium ion becomes much stronger (monodentate → bidentate → tridentate coordination) and the chemical shift of the ^{7}Li signal becomes much larger on subsequently going to molar ratios of [terpy]:[Li^+] = 1:1 and 1:2.

In Figure 4, the chemical shift of the ^{7}Li signal was plotted as a function of the molar ratio [terpy]:[Li^+]. As outlined by the blue data points (NMR spectra recorded at 25 °C), a break point in the chemical shift can be observed at a molar ratio of [terpy]:[Li^+] = 2:1. However, because of the significantly broadened signals at subequivalent concentration levels, the appropriate chemical shifts cannot be used for the construction of a straight line, and the resulting coordination number of two cannot be precisely determined. To resolve this complication, the measurements were repeated at 50 °C. Although the overall equilibrium between solvated and coordinated lithium ions (eq 1) is influenced by the elevated temperature, the signals at subequivalent concentrations became much sharper due to the accelerated exchange between the different lithium species. As shown by the red data points in Figure 4, the overall chemical shift of the ^{7}Li signal decreases significantly on increasing the temperature and the constructed line features a more distinct curvature. This leads to the conclusion that the complex-

dx.doi.org/10.1021/ic4020724 | Inorg. Chem. 2013, 52, 13167−13178

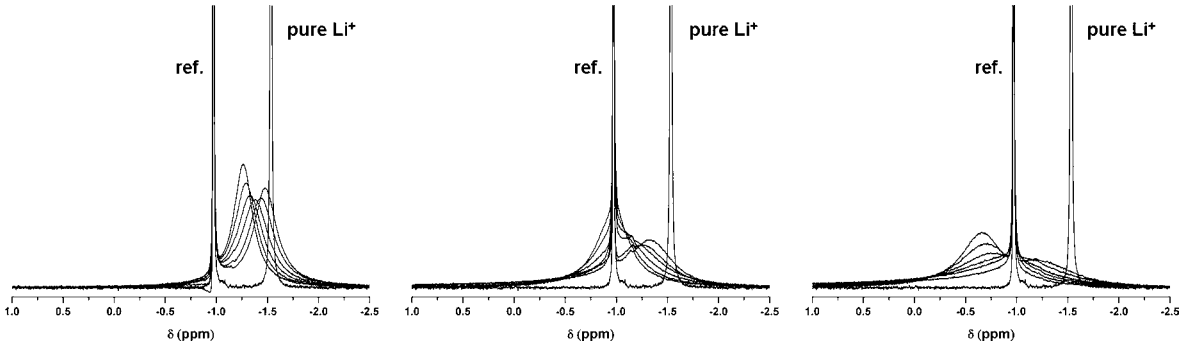

Figure 3. ^{7}Li NMR spectra recorded as a function of the temperature (25−50 °C) at subequivalent addition of terpy. From left to right: 0.1-, 0.2-, and 0.3-fold concentration of terpy compared to Li^+.

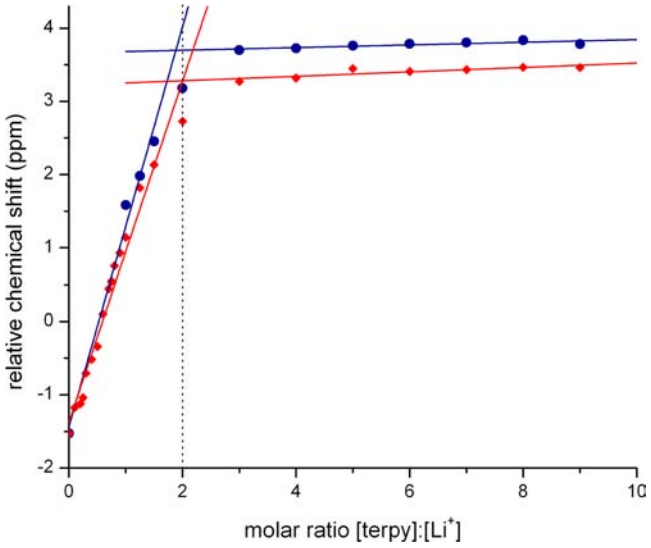

Figure 4. Chemical shift of the ^{7}Li signal as a function of the molar ratio [terpy]:[Li^+] in [emim][NTf_2] at 25 °C (blue) and 50 °C (red).

formation reaction between terpy and Li^+ is an exothermic process as the equilibrium between solvated and coordinated lithium ions is shifted to the reactant side on increasing the temperature (see also Table 1). Nevertheless, the crossing point of the red lines clearly indicates a discontinuity in the chemical shift at a molar ratio of [terpy]:[Li^+] = 2:1. Thus, a maximum of two terpy molecules can occupy the first coordination sphere of Li^+ in [emim][NTf_2] under the selected conditions.

$$Li^+ + 2\,terpy \rightleftarrows [Li(terpy)_2]^+ \quad (1)$$

Nevertheless, the question remains if both terpy molecules are really coordinated as tridentate ligands to generate the cationic complex $[Li(terpy)_2]^+$ in solution, or if to some extent, a solvent anion is coordinated to Li^+. From ESI mass spectrometry experiments performed in nitromethane, we were able to verify the existence of $[Li(terpy)_2]^+$ in solution.[31] Unfortunately, in the case of ILs, mass spectrometry failed because of the highly ionic nature of the solvent.

On applying quantum chemical calculations (B3LYP/LANL2DZp), we determined the energy differences between various partially coordinated $[Li(terpy)_2]^+$ complexes ranging from four occupied coordination sites on Li^+ (see Figures S1−4, Supporting Information) to completely saturated Li^+ (i.e., six occupied coordination sites). As compared to the 4-fold coordinated structure presented in Figure S1 (Supporting Information), we found a clear preference of −12.8 kcal/mol for the S_4 symmetric 6-fold coordinated $[Li(terpy)_2]^+$ complex shown in Figure 5. This leads to the conclusion that the first coordination sphere of Li^+ is saturated by two terpy molecules and the coordination of an additional anion can therefore be excluded.

Coordination of terpy to Li^+ in [emim][ClO_4]. Due to a complete delocalization of the negative charge, ClO_4^- anions exhibit a perfect tetrahedral structure and a low polarizability. As a consequence, they behave as poor nucleophiles with a low coordination ability and together with $[emim]^+$ cations, they generate a room temperature ionic liquid (RTIL) with a donor number of 7.6. Despite its low coordination ability, [emim]-[ClO_4] has a hydrophilic nature.[15,19,32] Therefore, this IL represents an interesting alternative to fluorinated ILs, such as [emim][BF_4] (DN = 7.3), which tend to undergo hydrolysis and generate hydrofluoric acid.

As expected from the NMR data obtained for [emim][NTf_2], the successive addition of terpy to a solution of $LiClO_4$ in [emim][ClO_4] likewise resulted in a significant downfield shift of the ^{7}Li NMR signal up to a molar ratio of [terpy]:[Li^+] = 4:1. However, at higher concentration levels, the ^{7}Li signal shows a clear drift, which points to a more distinct interaction between solvated and coordinated lithium ions as compared to [emim][NTf_2]. At subequivalent concentrations of terpy, the ^{7}Li spectra also exhibit significant line broadening (see Figure 6). Though these broad signals clearly indicate the presence of equilibria between different lithium ligated species, the exchange rate between these species seems to be much higher as compared to [emim][NTf_2], and the formation of intermediate species (i.e., more than one signal) cannot be seen from the spectra. This observation can be ascribed to the smaller size of ClO_4^- as compared to the sterically demanding NTf_2^- anion and the lower coordination ability of ClO_4^-. These effects lead to a much faster exchange between terpy and ClO_4^- on Li^+, which in turn will lower the stability of the resulting terpy complexes.

Although the signals at subequivalent concentrations of terpy are significantly broadened, they are still sufficient for the assignment of chemical shifts. In Figure 7 the chemical shift is plotted as a function of the molar ratio [terpy]:[Li^+]. As indicated by the blue data points (25 °C), the successive addition of terpy to Li^+ leads to more than only one discontinuity in the chemical shift and clear break-points can be observed at molar ratios of [terpy]:[Li^+] ≈ 1:1 and 2:1. This suggests that under these conditions, the different discontinuities reflect the stepwise addition of terpy, although the

dx.doi.org/10.1021/ic4020724 | Inorg. Chem. 2013, 52, 13167−13178

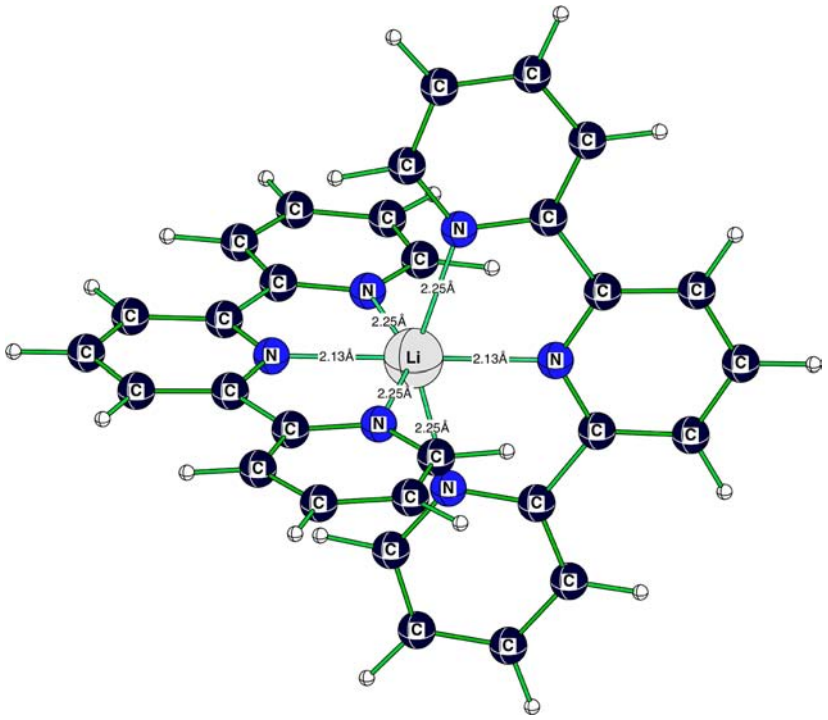

Figure 5. Calculated structure (B3LYP/LANL2DZp) of $[Li\ (terpy)_2]^+$.

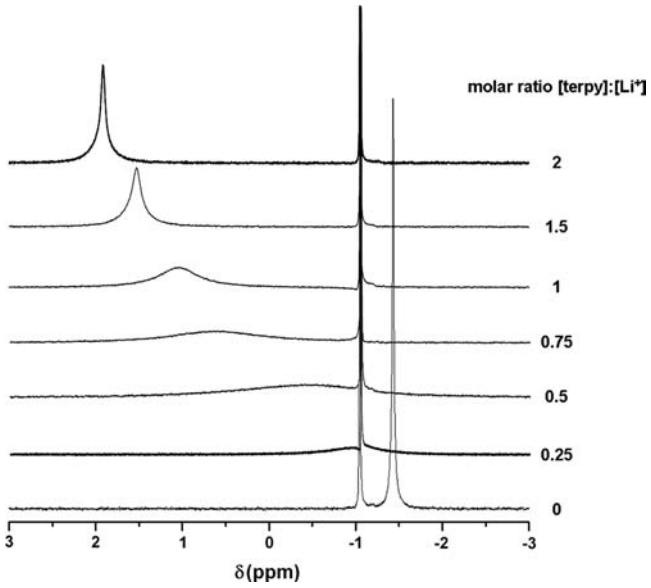

Figure 6. Selected ^{7}Li NMR spectra recorded as a function of the molar ratio [terpy]:$[Li^+]$ in $[emim][ClO_4]$ at 25 °C.

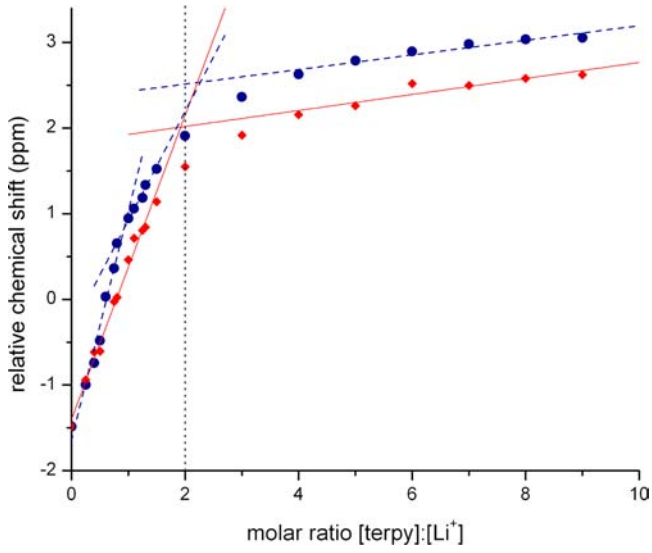

Figure 7. Chemical shift of the ^{7}Li signal as a function of the molar ratio [terpy]:$[Li^+]$ in $[emim][ClO_4]$ at 25 °C (blue) and 50 °C (red).

individual spectra only exhibit one signal. Other studies on the coordination of pyridine to Li^+ in $[emim][ClO_4]$ resulted in similar observations.[33] Here, at least three clear discontinuities were observed (see Figure S5, Supporting Information). To determine the coordination number of terpy more precisely, we repeated the measurements at 50 °C to obtain sharper signals as a result of faster ligand exchange reactions.

As seen from the red data points in Figure 7, an increase in the temperature leads to a clear decrease in the overall chemical shift. This behavior can again be ascribed to the exothermic nature of the complex-formation reaction. Therefore, the initial slope also becomes smaller on increasing the temperature, and the "intermediate" discontinuities become less distinct. However, the crossing point of the red lines clearly reveals the coordination of a maximum of two terpy molecules to generate $[Li(terpy)_2]^+$ under these conditions.

Stability Constants and Thermodynamics. As a result of the overall equilibrium (eq 1) between solvated and coordinated lithium ions, the plots presented in Figures 4 and 7 exhibit a clear curvature typical for a complex-formation reaction. Depending on the position of this equilibrium (i.e., either near to the reactant side or near to the product side) the NMR data differs more or less from the applied linear fits in the region of the observed discontinuities. On application of eq 2, these differences at a molar ratio of [terpy]:$[Li^+]$ = 2 can be used to estimate the overall stability constants β_2 of the

dx.doi.org/10.1021/ic4020724 | Inorg. Chem. 2013, 52, 13167−13178

Table 1. Overall Stability Constants β_2 for Li(terpy)$_2$ Complexes

complex	solvent	donor number	β_2 [M^{-2}]	log β_2	$\Delta H°$ [kJ/mol]	$\Delta S°$ [J/Kmol]
$[Li(terpy)_2]^+$	[emim][NTf$_2$]	11.2	$(156 \pm 10) \times 10^3$	5.19	-30.9 ± 0.1	-4.1 ± 0.3
$[Li(terpy)_2]^+$	[emim][ClO$_4$]	7.6	$(48 \pm 11) \times 10^3$	4.68	-6.9 ± 0.1	$+66.6 \pm 0.4$
$[Li(terpy)_2]^+$	nitromethane	2.7	$(635 \pm 204) \times 10^3$[a]	5.80	-24.3 ± 0.4	$+30 \pm 1$
$[Li(bipy)_2]^+$	[emim][NTf$_2$]	11.2	$(29 \pm 3) \times 10^3$[b]	4.46	-30.8 ± 0.1	$+18.1 \pm 0.3$
$[Li(bipy)_2]^+$	[emim][ClO$_4$]	7.6	$(28 \pm 3) \times 10^3$[b]	4.45	-26.4 ± 0.3	-3.5 ± 1
$[Li(bipy)_2]^+$	nitromethane	2.7	$(57 \pm 8) \times 10^3$[b]	4.76	-16.1 ± 0.3	$+37 \pm 1$

[a]This value was derived from the data reported in ref 31. [b]These values were derived from the data reported in ref 16.

generated $[Li(terpy)_2]^+$ complexes. The required concentrations of free terpy, free lithium, and chelated lithium can be calculated from the measured and expected chemical shifts and the total concentrations of Li^+ and terpy at this molar ratio:

$$\beta_2 = \frac{[Li(terpy)_2]}{[Li^+_{free}][terpy_{free}]^2} \quad (2)$$

According to eq 3, the temperature dependence of β_2 allows the determination of the standard reaction parameters $\Delta H°$ and $\Delta S°$. Therefore, the chemical shift of the ^{7}Li signal ([terpy]:[Li$^+$] = 2) was measured as a function of the temperature in the range 25−55 °C. A linear plot of ln β_2 versus $1/T$ enabled the calculation of $\Delta H°$ and $\Delta S°$ from the slope and intercept of the plot, respectively (e.g., see Figure S6, Supporting Information).

$$R \ln \beta_2 = -\frac{\Delta H°}{T} + \Delta S° \quad (3)$$

The resulting stability constants and standard reaction parameters are summarized in Table 1 and are compared to our earlier data on the coordination of bipy to Li^+.[16] In terms of the stability of the formed complex, β_2 in general increases on using terpy instead of bipy. This observation can be explained by the stronger chelate effect of the tridentate terpy ligand, which results from the additional N-donor atom. The largest increase in the complex stability of $[Li(terpy)_2]^+$ can be observed for the nonionic solvent nitromethane. Here, β_2 was found to be eleven times higher as compared to $[Li(bipy)_2]^+$. As a consequence of the low polarity and the low coordination ability of nitromethane, solvent−solute interactions are weak and the determined stability constants best reflect the influence of the chelate effect. Concerning the employed ILs, β_2 increases significantly more for [emim][NTf$_2$] than for [emim][ClO$_4$], despite the lower donor number of [emim][ClO$_4$]. As mentioned above, this effect originates from the smaller size of the perchlorate anion and its lower coordination ability. Both lead to a much faster exchange between terpy and ClO_4^- on Li^+ and, thus, to a lower stability of $[Li(terpy)_2]^+$ in [emim][ClO$_4$]. A similar observation can be made in terms of $[Li(bipy)_2]^+$. Although for both ILs, the observed stability constants range in the same order of magnitude, β_2 should be definitely higher for [emim][ClO$_4$] with respect to the lower donicity of this solvent. Nevertheless, the data clearly show that the complex stability generally decreases on applying ionic reaction media. Besides a specific influence of the appropriate anions of an IL, such as Lewis basicity or sterical hindrance, this observation can be attributed to stronger solvent−solute interactions as a consequence of the ionic character and the higher polarity.

In agreement with our experimental observations that the overall chemical shift becomes smaller on increasing the temperature, the determination of the standard reaction parameters according to eq 3 resulted in negative values for $\Delta H°$, viz. an exothermic complex-formation reaction. At first glance, the standard reaction enthalpy of $\Delta H° = -6.9 \pm 0.1$ kJ mol^{-1} for the formation of $[Li(terpy)_2]^+$ in [emim][ClO$_4$] seems to be small compared to the other data. However, this small value can be accounted for in terms of the high lability of the system as a consequence of the fast exchange between terpy and ClO_4^- on Li^+. The activation enthalpy $\Delta H^‡$ of both the forward and the backward reactions in eq 1 seem to be of the same order of magnitude, thus resulting in the small value of $\Delta H°$. On the contrary, this system exhibits an exceptionally high standard reaction entropy of $\Delta S° = +66.6 \pm 0.4$ J K^{-1} mol^{-1}. This suggests that the formation of $[Li(terpy)_2]^+$ in [emim][ClO$_4$] is an entropy driven process. Notably, the same reaction behaves the other way around on using [emim][NTf$_2$] as the solvent. Here, the standard reaction enthalpy $\Delta H° = -29.9 \pm 0.1$ kJ mol^{-1} was found to be large, whereas the standard reaction entropy $\Delta S° = -4.1 \pm 0.3$ J K^{-1} mol^{-1} was found to be close to zero. Therefore, complex formation of $[Li(terpy)_2]^+$ becomes an enthalpy driven process on applying [emim][NTf$_2$] instead of [emim][ClO$_4$] (see Figure S7, Supporting Information).

In contrast to the nonionic solvent nitromethane, lithium ions, or more generally speaking metal ions, dissolved in ILs exhibit an anionic solvent shell. Thus, the complex-formation reaction involves a change in the overall charge on going from $[Li(anion)_n]^{-(n-1)}$ to $[Li(terpy)_2]^+$ and leads to a spreading out of the second coordination sphere on Li^+. For the standard reaction parameters $\Delta H°$ and $\Delta S°$, one should keep in mind that especially the value of the reaction entropy is affected by contributions from bonding and solvation effects, which originate from changes in the charge of a complex. Although our values of $\Delta S°$ are also influenced by these effects, the large difference between $\Delta S°$ determined for the formation of $[Li(terpy)_2]^+$ in [emim][NTf$_2$] and in [emim][ClO$_4$] can also be explained by the number of solvent anions substituted during the complex-formation process. In the case of [emim][NTf$_2$], two solvent anions were found to occupy the first coordination sphere of Li^+.[30] Therefore, the complex-formation reaction of $[Li(terpy)_2]^+$ involves substitution of two solvent anions by two ligand molecules. In total, there is no change in the number of free molecules which would lead to an increase in the disorder of the system. Unfortunately, there is no clear information available on how many ClO_4^- anions are coordinated to Li^+ in [emim][ClO$_4$]. Although most studies on related systems indicate that Li^+ is 4-fold coordinated in solution,[34] Wickleder as well as Henderson et al. published a crystal structure of lithium ions coordinated in an octahedral geometry by six monodentate bound ClO_4^- anions.[35] On considering a number of four to six ClO_4^- anions that occupy the first coordination sphere of Li^+ dissolved in [emim][ClO$_4$], the formation of $[Li(terpy)_2]^+$ involves the displacement of four to six solvent anions by two ligand molecules. In total, the

dx.doi.org/10.1021/ic4020724 | Inorg. Chem. 2013, 52, 13167−13178

number of free molecules increases by two to four per lithium ion, which will lead to a significant increase in the disorder of the system, and therefore to a higher value of $\Delta S°$.

In terms of our earlier work on the formation of $[Li(bipy)_2]$, the interpretation of the standard reaction entropy is significantly more difficult. Due to the smaller size of the bipy ligand, the first coordination sphere of Li^+ is not completely saturated and the coordination (or at least partial coordination) of one or more solvent anions should be considered.

X-ray Diffraction Studies. The crystals used for X-ray diffraction studies were obtained directly from the employed ionic liquids. Similar to our ^{7}Li NMR experiments and to exclude possible effects of other anions, we used lithium salts, which involved the same anionic component as compared to the employed ILs. Important details and parameters concerning the data collection and structure refinements are given in Table 2.

Table 2. Crystallographic Data, Data Collection, and Refinement Details for the Investigated Compounds

CSD-ref code	CCDC-954465	CCDC-954464
substance	$[\{Li(terpy)(NTf_2)\}]_n$	$[Li(terpy)(ClO_4)]_2$
empirical formula	$C_{17}H_{11}LiN_4O_4F_6S_2$	$C_{30}H_{22}Li_2N_6O_8Cl_2$
mol weight (g/mol)	520.36	676.32
crystal size (mm^3)	0.29 × 0.21 × 0.18	0.34 × 0.24 × 0.07
temperature (K)	173.00(10)	173.00
crystal system	monoclinic	triclinic
space group	$P2_1/n$	$P\bar{1}$
a (Å)	9.7851(2)	8.6325(7)
b (Å)	17.2371(4)	9.6777(11)
c (Å)	13.0780(3)	10.5904(9)
α (deg)	90.00	103.254(8)
β (deg)	101.160(2)	108.437(8)
γ (deg)	90.00	108.812(9)
V ($Å^3$)	2164.11(9)	738.47(12)
Z	4	1
ρ (mg/mm^3) (calcd)	1.597	1.528
μ (mm^{-1})	0.330	0.284
$F(000)$	1048.0	348.0
abs corr	analytical	analytical
T_{min}; T_{max}	0.983; 0.986	0.956; 0.990
2Θ interval (deg)	6.24 ≤ 2Θ ≤ 52.74	6.7 ≤ 2Θ ≤ 50.1
coll refln	7200	3682
Indep refln	4388	2600
R(int)	0.0322	0.0189
obs refln $[I \geq 2\sigma(I)]$	3546	2085
no. ref param	307	217
wR_2 (all data)	0.1155	0.1132
R_1 $[I \geq 2\sigma(I)]$	0.0438	0.0427
GOF F^2	1.046	1.043
max; min res electr density (e $Å^{-3}$)	+0.29; −0.46	+0.49; −0.39

Structure of $[Li(terpy)(NTf_2)]_n$ (1). Although all crystals were grown with a 3-fold excess of terpy over Li^+, X-ray diffraction analysis revealed a completely different coordination number and pattern in the solid state, as compared to the results of the ^{7}Li NMR measurements. The polymeric lithium species $[Li(terpy)(NTf_2)]_n$ (**1**) was found to be the principal structural motif, in which each Li^+ cation is coordinated by only one terpy ligand. The asymmetric unit of **1** contains a Li^+ cation bound by one terpy molecule and one NTf_2^- anion (see Figure 8).

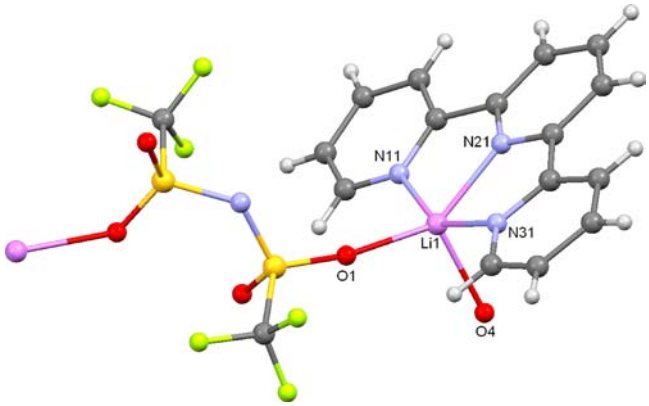

Figure 8. Molecular structure of $[Li(terpy)(NTf_2)]_n$ (**1**).

All in all, each Li^+ cation is 5-fold coordinated by two oxygen and three nitrogen donor atoms. Applying the concept of Addison and Reedijk,[36] who introduced the so-called τ value ($\tau = (\beta - \alpha)/60$) to characterize the geometry of five-coordinate complexes, we found that the basal angles of α = 146.0 (2)° (O(1)−Li(1)−N(21)) and β = 151.2 (2)° (N(11)−Li(1)−N(31)) result in a τ value of 0.09, which indicates a slightly distorted square-pyramidal coordination geometry. The polymeric character of **1** arises from the bridging of neighboring Li^+ centers by NTf_2^- anions. Considering the stacking (see Figure 9), **1** is arranged in antiparallel chains running parallel to the *ac*-plane, along the vector $(\vec{a} + \vec{c})$. Due to the antiparallel orientation of **1**, terpy ligands of neighboring chains face each other, and average distances of 3.67 Å (determined as the distance between the centers of neighboring C26−C32 bonds) enable $\pi-\pi$ interactions between parts of these ligands.

In terms of the NTf_2^- anions, the trifluoromethyl groups of the anion are oriented in opposite directions. Considering the stacking, this transoid orientation enables the formation of the so-called "fluorous regions", typical for crystal structures involving NTf_2^- anions.[16,37] In the present case, these hydrophobic arrays run along the *a*-axis between the polymeric chains and separate the regions of π-stacking (see Figure 10).

As mentioned in our earlier work,[16] the NTf_2^- anion exhibits a clear preference for coordination via oxygen atoms. This can, on the one hand, be attributed to steric effects and on the other hand, to the electron withdrawing character of the trifluoromethyl groups, which leads to a lack of electron density on the imide nitrogen atom.[16,38,39] Interestingly, NTf_2^- behaves in this case only as a bis-monodentate ligand bridging the individual Li^+ ions with trans-positioned oxygen atoms of different sulfonyl subunits. This observation can be ascribed to the strong chelate effect of the terpy ligand and the sterical demanding nature of the NTf_2^- anion. In contrast to our earlier work,[16] where the NTf_2^- anion together with Li^+ and bipyridine, was found to generate a discrete dimeric species (see Figure S8, Supporting Information). In the present case, the required additional coordination site at the lithium center is already occupied by the third N-donor atom of the terpy ligand and, in addition, the NTf_2^- anion is much too voluminous to generate a similar dimeric lithium species as observed for bipyridine.

dx.doi.org/10.1021/ic4020724 | Inorg. Chem. 2013, 52, 13167−13178

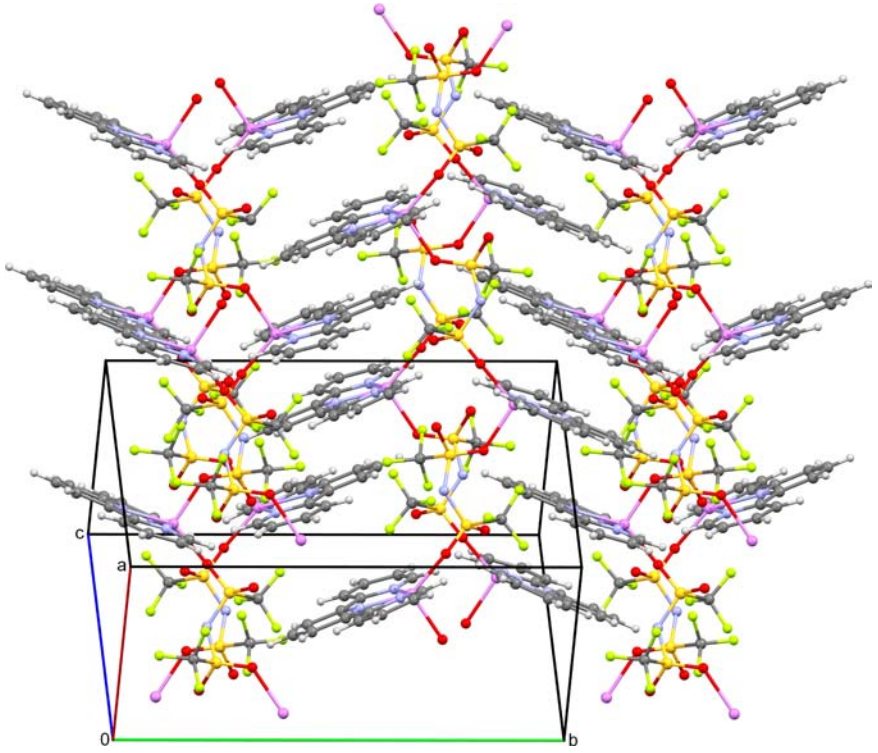

Figure 9. Stacking of $[Li(terpy)(NTf_2)]_n$ (**1**), view on *b* along the vector $(\vec{a} - \vec{c})$.

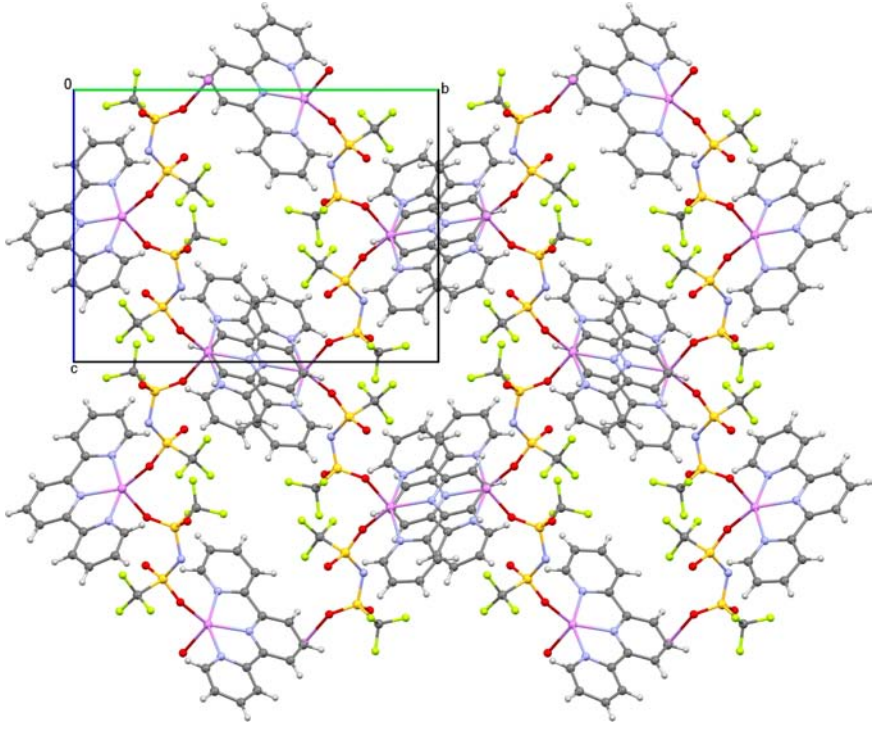

Figure 10. Stacking of $[Li(terpy)(NTf_2)]_n$ (**1**), view along the crystallographic *a*-axis. A typical "fluorous region" is highlighted by the axes of the elementary cell.

Structure of $[Li(terpy)(ClO_4)]_2$ (2). Similar to the crystal structure found for the coordination of terpy to Li^+ in $[emim][NTf_2]$, X-ray diffraction studies on crystals grown from $[emim][ClO_4]$ likewise revealed the coordination of only one terpy molecule per lithium ion. However, the overall coordination pattern was found to be completely different. In contrast to **1**, a discrete dimeric species was found to be the principal structural motif that exhibits the empirical formula $[Li(terpy)(ClO_4)]_2$ (**2**) (see Figure 11). The asymmetric unit of **2** contains one-half of the molecule, whereas the second half is generated by an inversion center, located at the center of the molecule.

dx.doi.org/10.1021/ic4020724 | *Inorg. Chem.* 2013, 52, 13167−13178

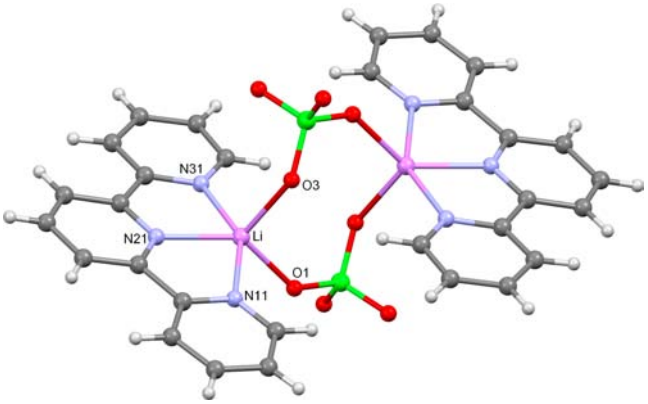

Figure 11. Molecular structure of $[Li(terpy)(ClO_4)]_2$ (**2**).

Within this dimer, the individual lithium ions are 5-fold coordinated by two oxygen and three nitrogen donor atoms. Basal angles of α = 136.7 (2)° (O(1)−Li(1)−N(21)) and β = 150.5 (2)° (N(11)−Li(1)−N(31)) result in a τ value of 0.23, indicating a distorted square-pyramidal coordination geometry. Both lithium centers are doubly bridged by two perchlorate anions (μ-perchlorato), each of them occupying the apical position of one polyhedron and one of the square-base positions of the other polyhedron.

As shown in Figure 12, the dimers are arranged as layers of indented parallel chains, which run along the *a*-axis. Within one chain, **2** is placed in a slightly staggered position to the dimers of the next chain. Due to this arrangement, the terpy ligands of dimers of neighboring chains face each other, and average distances of 3.73 Å (determined as the distance between the centers of the neighboring C26−C32 bonds) enable $\pi-\pi$ interactions between parts of these ligands. In terms of the same chain, the terpy ligands overlap only slightly and the effect of $\pi-\pi$ interactions is very small. Considering the stacking in the third dimension, Figure 13 shows that the individual layers are also indented through partial overlapping of the terpy ligands. As a consequence of the symmetry, average distances of 3.51 Å (determined as the distance between the centers of the neighboring C14−C15 and C16−C22 bonds) lead to slightly stronger $\pi-\pi$ interactions between the layers as compared to the interactions within one layer.

Notably, in our previous work on the coordination of bipy to Li^+ we obtained a very similar dimeric lithium species in the case of the IL $[emim][NTf_2]$ (see Figure S8, Supporting Information).[16] Due to the fact that both **1** and **2** were grown under the same conditions, but **1** exhibits a completely different structural pattern, it can be concluded that besides steric or size effects, the interplay between ligand and anion nature mainly controls the formation of the dimeric species. Considering the nature of the anionic component, the anions must at least be able to act as bridging ligands, otherwise a dimerization would not be possible. In the case of **2**, the tridentate terpy ligand is much larger as compared to the bidentate bipy ligand. However, in terms of the formation of the dimeric species, the larger size of the terpy ligand is compensated by the smaller size of the ClO_4^- anion. A similar observation can be made with respect to the occupied coordination sites. Although the terpy ligand requires an additional coordination site on Li^+, this site is in principle provided by the ClO_4^- anion. Due to its tetrahedral structure, ClO_4^- can only act as bidentate or bridging ligand; compared to the structure presented in Figure S7 (Supporting Information), one coordination site on Li^+ is not used and can therefore be occupied by the third N-donor atom of the terpy ligand. To prove whether the formation of the dimeric species is to some extent favored by packing effects such as π-stacking or C−H···O interactions, we calculated the structure of **2** without any symmetry constraints applying DFT methods (B3LYP/LANL2DZp). Although the exact values of the distances, torsions and angles were found to be affected by the stacking process, the results clearly showed that dimer **2** is stable as an isolated molecule in the gas phase (see Figure S9, Supporting Information).

CONCLUSIONS

In this work, we studied the complex-formation reaction between lithium ions and terpy, employing the ILs $[emim][NTf_2]$ and $[emim][ClO_4]$ as solvents. The results obtained from the ^{7}Li NMR data clearly demonstrate that a maximum of two terpy molecules can occupy the first coordination sphere of

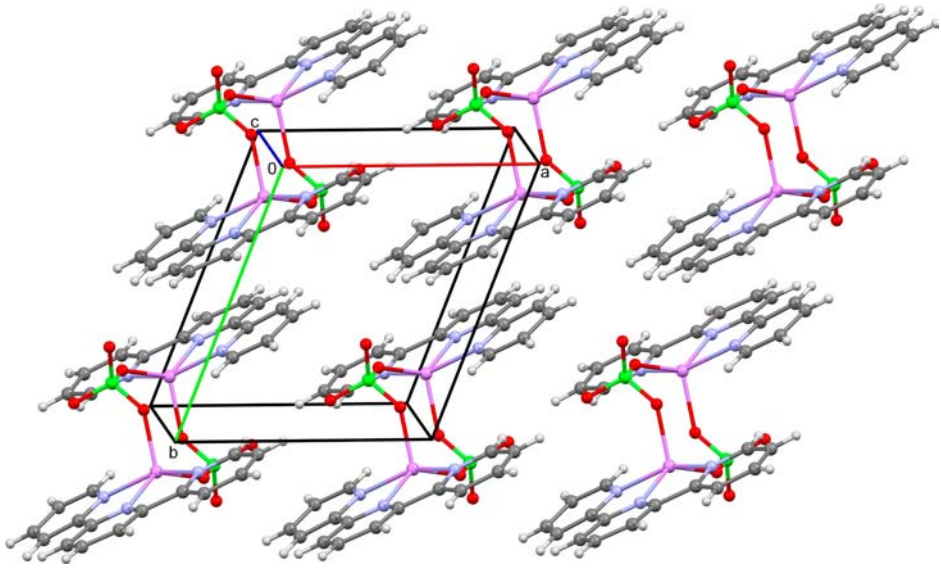

Figure 12. Stacking of $[Li(terpy)(ClO_4)]_2$ (**2**), view along the crystallographic *c*-axis (top-view on a monolayer).

dx.doi.org/10.1021/ic4020724 | *Inorg. Chem.* 2013, 52, 13167−13178

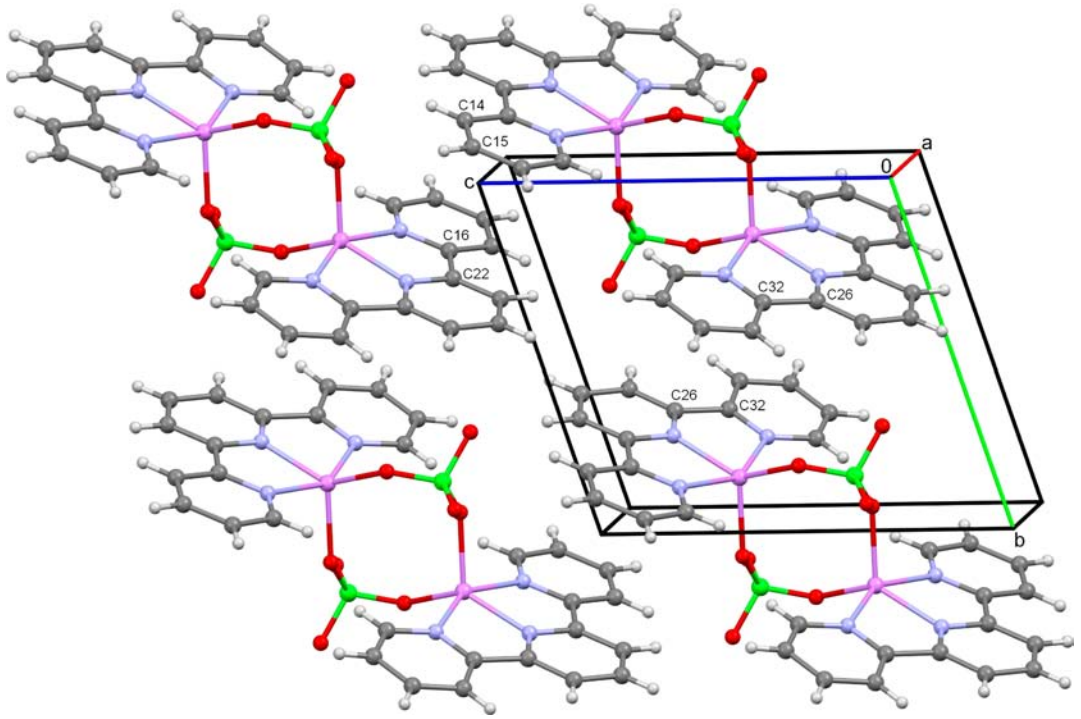

Figure 13. Stacking of $[Li(terpy)(ClO_4)]_2$ (**2**), view along the crystallographic *a*-axis (side-view on two layers).

Li^+ to generate the cationic complex $[Li(terpy)_2]^+$ in solution. With respect to our earlier work,[16] the application of the tridentate terpy ligand resulted in a significant increase in the stability of $[Li(terpy)_2]^+$ as compared to $[Li(bipy)_2]^+$. However, the data also showed that in contrast to the nonionic solvent nitromethane, in the case of ILs, stronger solvent−solute interactions generally reduce the complex stability. Notably, the smaller size of the ClO_4^- anion and its less sterical demanding structure lead to a higher competition between terpy and ClO_4^- on Li^+ and to a stronger decrease in complex stability in $[emim][ClO_4]$ as compared to $[emim][NTf_2]$. Thus, a complex-formation reaction must not necessarily be favored, on applying a solvent with a lower donicity. In terms of the determined standard reaction parameters $\Delta H°$ and $\Delta S°$, the complex formation of $[Li(terpy)_2]^+$ was found to be enthalpy driven in $[emim][NTf_2]$, whereas in the case of $[emim][ClO_4]$ the same process was found to be entropy driven. Therefore, it can be concluded that on applying ILs as reaction media, the driving force of a chemical process can significantly be affected by the nature of the anionic component of an IL, although the anionic component is known to be a weak Lewis base.

In contrast to the NMR data, X-ray diffraction measurements on isolated crystals showed that each lithium ion is formally coordinated by only one terpy molecule and one solvent anion (polymeric as well as dimeric species) suggesting that charge neutralization and π-stacking mainly control the crystallization process. As a consequence, the cationic $[Li(terpy)_2]^+$ complex was only stable in solution and could not be isolated as a $[Li(terpy)_2]^+[anion]^-$ salt from the employed ILs under these conditions.

In general, it can be concluded that our understanding of how metal salts dissolve in ionic liquids, and how ionic liquids actually interact with catalytically active metal complexes, still remains rather limited. Although a good understanding of the role of conventional solvents has been developed, much more remains to be done to reach such an understanding in the case of ionic liquids.

■ ASSOCIATED CONTENT

Supporting Information

Three calculated structures of $[Li(terpy)_2]^+$ with four occupied coordination sites at Li^+, a calculated structure of $[Li(terpy)_2]^+$ with five occupied coordination sites at Li^+, the chemical shift of the ^7Li signal as a function of the added pyridine concentration, plot of ln β_2 versus $1/T$ to determine $\Delta H°$ and $\Delta S°$ of the formation of $[Li(terpy)_2]^+$ in $[emim][NTf_2]$, compensation-relationship between $\Delta H°$ and $\Delta S°$ determined for the formation of $[Li(terpy)_2]^+$, molecular structure of $[Li(bipy)(NTf_2)]_2$, and calculated structure of $[Li(terpy)(ClO_4)]_2$. This material is available free of charge via the Internet at http://pubs.acs.org.

■ AUTHOR INFORMATION

Corresponding Author

*R. van Eldik. E-mail: vaneldik@chemie.uni-erlangen.de.

Notes

The authors declare no competing financial interest.

■ ACKNOWLEDGMENTS

The authors gratefully acknowledge continued financial support from the Deutsche Forschungsgemeinschaft.

■ REFERENCES

(1) (a) Wilkes, J. S. In *Ionic liquids in Synthesis*; Wasserscheid, P., Welton, T., Eds.; Wiley-VCH: Weinheim, 2008, Introduction. (b) Weigärtner, H. *Angew. Chem., Int. Ed.* **2008**, *47*, 654−670. (c) Wasserscheid, P. *ChiuZ* **2003**, *37*, 52−63. (d) Wasserscheid, P.; Keim, W. *Angew. Chem., Int. Ed.* **2000**, *39*, 3772−3789.

(2) (a) Tariq, M.; Carvalho, P. J.; Coutinho, J. A. P.; Marrucho, I. M.; Canongia Lopes, J. N.; Rebelo, L. P. N. *Fluid Phase Equilib.* **2011**, *301*, 22−32. (b) Harris, K. R.; Kanakubo, M.; Woolf, L. A. *J. Chem. Eng.*

Data **2007**, *52*, 1080−1085. (c) Tokuda, H.; Hayamizu, K.; Ishii, K.; Abu Bin, H.; Susan, M. A.; Watanabe, M. *J. Phys. Chem. B* **2005**, *109*, 6103−6110. (d) Roland, C. M.; Bair, S.; Casalini, R. *J. Chem. Phys.* **2006**, *125*, 124508−124508-8. (e) Harris, K. R.; Woolf, L. A.; Kanakubo, M. J. *Chem. Eng. Data* **2005**, *50*, 1777−1782.

(3) (a) Doherty, S.; Goodrich, P.; Hardacre, C.; Parvulescu, V.; Paun, C. *Adv. Synth. Catal.* **2008**, *350*, 295−302. (b) Abbott, A. P.; Dalrymple, I.; Endres, F.; McFarlane, D. R. In *Electrodeposition from Ionic liquids*; Endres, F., Abbot, A. P., McFralane, R., Eds.; Wiley-VCH: Weinheim, Germany, 2008; Chapter 1. (c) Paczal, A.; Kotschy, A. *Monatsh. Chem.* **2007**, *138*, 1115−1123. (d) Maase, M. In *Multiphase Homogeneous Catalysis*, Cornils, B., Herrmann, W. A., Horvath, I. T., Leitner, W., Mecking, S., Olivier-Bourbigou, H., Vogt, D., Eds.; Wiley-VCH: Weinheim, Germany, 2005; Vol. *2*, pp 560−566; (e) Freemantle, M. *Chem. Eng. News* **2003**, *81*, 9. (f) Rogers, R.; Seddon, K. R. *Science* **2003**, *302*, 792−793. (g) Bösmann, A.; Francio, G.; Janssen, E.; Solinas, M.; Leitner, W.; Wasserscheid, P. *Angew. Chem.* **2001**, *113*, 2769−2771. (h) Sheldon, R. *Chem. Commun.* **2001**, *23*, 2399−2407.

(4) (a) Earle, M. J.; Hakala, U.; McAuley, B. J.; Nieuwnhuyzen, M.; Ramani, A.; Seddon, K. R. *Chem. Commun.* **2004**, *12*, 1368−1369. (b) Magna, L.; Chauvin, Y.; Niccolai, G. P.; Basset, J. M. *Organometallics* **2003**, *22*, 4418−4425.

(5) (a) Mc. Nulty, J.; Cheekoori, S.; Bender, T. P.; Coggan, J. A. *Eur. J. Org. Chem.* **2007**, *9*, 1423−1428. (b) Daguenet, C.; Dyson, P. *Organometallics* **2006**, *25*, 5811−5816. (c) Schmeisser, M.; van Eldik, R. *Inorg. Chem.* **2009**, *48*, 7466−7475.

(6) Hubbard, C. D.; Illner, P.; van Eldik, R. *Chem. Soc. Rev.* **2011**, *40*, 272−290.

(7) (a) Ciappe, C.; Pomelli, C. S.; Rajamani, S. *J. Phys. Chem. B* **2011**, *115*, 9653−9661. (b) Ab Rani, M. A.; Brant, A.; Crowhurst, L.; Dolan, A.; Lui, M.; Niedermeyer, H.; Perez-Arlandis, J. M.; Schrems, M.; Welton, T.; Wilding. *Phys. Chem. Chem. Phys.* **2011**, *13*, 16831−16840. (c) Doherty, T. V.; Mora-Pale, M.; Foley, S. E.; Lienhardt, R. J.; Dordick, J. S. *Green Chem.* **2010**, *12*, 1967−1975. (d) Chiappe, C.; Pieraccini, D. *J. Phys. Org. Chem.* **2005**, *18*, 275−297. (e) Llewellyn, N.; Welton, T. *J. Org. Chem.* **2004**, *69*, 5986−5992. (f) Crowhurst, L.; Mawdsley, P. R.; Perez-Arlandis, J. M.; Salter, P. A.; Welton, T. *Phys. Chem. Chem. Phys.* **2003**, *5*, 2790−2794.

(8) (a) Lungwitz, R.; Strehmel, V.; Spange, S. *New J. Chem.* **2010**, *34*, 1135−1140. (b) Lungwitz, R.; Friedrich, M.; Linert, W.; Spange, S. *New J. Chem.* **2008**, *32*, 1493−1499. (c) Lungwitz, R.; Spange, S. *New J. Chem.* **2008**, *32*, 392−394.

(9) (a) Henderson, W. A.; Brooks, N. R.; Brennessel, W. W.; Young, V. G. *Chem. Mater.* **2003**, *15*, 4679−4684. (b) Henderson, W. A.; Brooks, N. R.; Young, V. G. *Chem. Mater.* **2003**, *15*, 4685−4690. (c) Henderson, W. A.; Passserini, S. *Chem. Mater.* **2004**, *16*, 2881−2885. (d) Castriota, M.; Caruso, T.; Agostino, R. G.; Cazzanelli, E.; Henderson, W. A.; Passserini, S. *J. Phys. Chem. A* **2005**, *109*, 92−96. (e) Henderson, W. A.; McKenna, F.; Khan, M. A.; Brooks, N. R.; Young, V. G.; Frech, R. *Chem. Mater.* **2005**, *17*, 2284−2289. (f) Zhou, Q.; Henderson, W. A.; Appetecchi, G. B.; Passserini, S. *J. Phys. Chem. C* **2010**, *114*, 6201−6204. (g) Zhou, Q.; Fitzgerald, K.; Boyle, P. D.; Henderson, W. A. *Chem. Mater.* **2010**, *22*, 1203−1208. (h) Zhou, Q.; Boyle, P. D.; Malpezzi, L.; Mele, A.; Shin, J.-H.; Passerini, S.; Henderson, W. A. *Chem. Mater.* **2011**, *23*, 4331−4337. (i) Han, S.-D.; Allen, J. L.; Jónsson, E.; Johansson, P.; McOwen, D. W.; Boyle, P. D.; Henderson, W. A. *J. Phys. Chem. C* **2013**, *117*, 5521−5531.

(10) (a) Shobukawa, H.; Tokuda, H.; Tabata, S.-I.; Watanabe, M. *Electrochim. Acta* **2004**, *50*, 305−309. (b) Seki, S.; Kobayashi, Y.; Miyashiro, H.; Ohno, Y.; Usami, A.; Mita, Y.; Watanabe, M. *Chem. Commun.* **2006**, *5*, 544−545. (c) Seki, S.; Kobayashi, Y.; Miyashiro, H.; Ohno, Y.; Usami, A.; Mita, Kihira, N.; Watanabe, M.; Terada, N. *J. Phys. Chem. B* **2006**, *110*, 10228−10230. (d) Seki, S.; Ohno, Y.; Kobayashi, Y.; Miyashiro, H.; Usami, A.; Mita, Y.; Tokuda, H.; Watanabe, M.; Hayamizu, K.; Tsuzuki, S. *J. Electrochem. Soc.* **2007**, *154*, A173−A177. (e) Seki, S.; Ohno, Y.; Miyashiro, H.; Kobayashi, Y.; Usami, A.; Mita, Y.; Terada, N.; Hayamizu, K.; Tsuzuki, S.; Watanabe, M. *J. Electrochem. Soc.* **2008**, *155*, A421−A427. (f) Tamura, T.; Yoshida, K.; Hachida, T.; Tsuchiya, M.; Nakamura, M.; Kazue, Y.; Tachikawa, N.; Dokko, K.; Watanabe, M. *Chem. Lett.* **2010**, *39*, 753−755. (g) Park, J.-W.; Yoshida, K.; Tachikawa, N.; Dokko, K.; Watanabe, M. *J. Power Sources* **2011**, *196*, 2264−2268. (h) Umebayashi, Y.; Hamano, H.; Seki, S.; Minofar, B.; Fujii, K.; Hayamizu, K.; Tsuzuki, S.; Kameda, Y.; Kohara, S.; Watanabe, M. *J. Phys. Chem. B* **2011**, *115*, 12179. (i) Ueno, K.; Yoshida, K.; Tsuchiya, M.; Tachikawa, N.; Dokko, K.; Watanabe, M. *J. Phys. Chem. B* **2012**, *116*, 11323−11331.

(11) (a) Mariappan, C. R.; Govindaraj, G.; Roling, B. *Solid State Ionics* **2005**, *176*, 723−729. (b) Taskiran, A.; Schirmeisen, A.; Fuchs, H.; Bracht, H.; Roling, B. *Phys. Chem. Chem. Phys.* **2009**, *11*, 5499−5505.

(12) Kern, S.; van Eldik, R. *Inorg. Chem.* **2012**, *51*, 7340−7345.

(13) (a) Begel, S.; van Eldik, R. *Dalton Trans.* **2011**, *40*, 4892−4897. (b) Begel, S.; Heinemann, F. W.; Stopa, G.; Stochel, G.; van Eldik, R. *Inorg. Chem.* **2011**, *50*, 3946−3958. (c) Schmeisser, M.; van Eldik, R. *Inorg. Chem.* **2009**, *48*, 7466−7475.

(14) (a) Kern, S.; Illner, P.; Begel, S.; van Eldik, R. *Eur. J. Inorg. Chem.* **2010**, *29*, 4658−4666. (b) Illner, P.; Begel, S.; Kern, S.; Puchta, R.; van Eldik, R. *Inorg. Chem.* **2009**, *48*, 588−597. (c) Begel, S.; Illner, P.; Kern, S.; Puchta, R.; van Eldik, R. *Inorg. Chem.* **2008**, *47*, 7121−7132. (d) Illner, P.; Kern, S.; Begel, S.; van Eldik, R. *Chem. Commun.* **2007**, *45*, 4803−4805.

(15) Schmeisser, M.; Illner, P.; Puchta, R.; Zahl, A.; van Eldik, R. *Chem.—Eur. J.* **2012**, *18*, 10969−10982.

(16) (a) Schmeisser, M.; Heinemann, F. W.; Illner, P.; Puchta, R.; Zahl, A.; van Eldik, R. *Inorg. Chem.* **2011**, *50*, 6685−6695. (b) Schmeisser, M.; Zahl, A.; Scheurer, A.; Puchta, R.; van Eldik, R. *Z. Naturforsch., B: J. Chem. Sci.* **2010**, *65*, 405−413.

(17) (a) Chiappe, C.; Pieraccini, D.; Zhao, D.; Fei, Z.; Dyson, P. J. *Adv. Synth. Catal.* **2006**, *348*, 68−74. (b) Bösmann, A.; Francio, G.; Janssen, E.; Solinas, M.; Leitner, W.; Wasserscheid, P. *Angew. Chem., Int. Ed.* **2001**, *40*, 2697−2699.

(18) Bonhôte, P.; Dias, A.-P.; Papageorgiou, N.; Kalyanasundaram, K.; Grätzel, M. *Inorg. Chem.* **1996**, *35*, 1168−1178.

(19) Schmeisser, M.; Keil, P.; Stierstorfer, J.; Koenig, A.; Klapötke, T. M.; van Eldik, R. *Eur. J. Inorg. Chem.* **2011**, 4862−4868.

(20) Klapötke, T. M.; Stierstorfer, J.; Brooke Jenkins, H. D.; van Eldik, R.; Schmeisser, M. *Z. Anorg. Allg. Chem.* **2011**, *637*, 1308−1313.

(21) Dolomanov, O. V.; Bourhis, L. J.; Gildea, R. J.; Howard, J. A. K.; Puschmann, H. *J. Appl. Crystallogr.* **2009**, *42*, 339−341.

(22) SHELXS, SHELXL, see: Sheldrick, G. M. *Acta Crystallogr., Sect. A* **2008**, *64*, 112−122.

(23) (a) Becke, A. D. *J. Chem. Phys.* **1993**, *98*, 5648−5652. (b) Lee, C.; Yang, W.; Parr, R. G. *Phys. Rev. B* **1988**, *37*, 785−789. (c) Stephens, P. J.; Devlin, F. J.; Chabalowski, C. F.; Frisch, M. J. *J. Phys. Chem.* **1994**, *98*, 11623−11627.

(24) (a) Hay, P. J.; Wadt, W. R. *J. Chem. Phys.* **1985**, *82*, 270−283. (b) Hay, P. J.; Wadt, W. R. *J. Chem. Phys.* **1985**, *82*, 284−298. (c) Hay, P. J.; Wadt, W. R. *J. Chem. Phys.* **1985**, *82*, 299−310.

(25) Huzinaga, S.; Andzelm, J.; Klobukowski, M.; Radzi-Andzelm, E.; Sakai; Y.; Tatewaki, H. in *Gaussian Basis Sets for Molecular Calculations*, Elsevier: Amsterdam, 1984.

(26) The performance of this method is well documented; see for example ref 12 and the references cited therein.

(27) Frisch, M. J.; Trucks, G. W.; Schlegel, H. B.; Scuseria, G. E.; Robb, M. A.; Cheeseman, J. R.; Montgomery, J. A., Jr.; Vreven, T.; Kudin, K. N.; Burant, J. C.; Millam, J. M.; Iyengar, S. S.; Tomasi, J.; Barone, V.; Mennucci, B.; Cossi, M.; Scalmani, G.; Rega, N.; Petersson, G. A.; Nakatsuji, H.; Hada, M.; Ehara, M.; Toyota, K.; Fukuda, R.; Hasegawa, J.; Ishida, M.; Nakajima, T.; Honda, Y.; Kitao, O.; Nakai, H.; Klene, M.; Li, X.; Knox, J. E.; Hratchian, H. P.; Cross, J. B.; Bakken, V.; Adamo, C.; Jaramillo, J.; Gomperts, R.; Stratmann, R. E.; Yazyev, O.; Austin, A. J.; Cammi, R.; Pomelli, J. W. Ochterski, P. Y. Ayala, K. Morokuma, G. A. Voth, P. Salvador, J. J. Dannenberg, V. G. Zakrzewski, S. Dapprich, C.; Daniels, A. D.; Strain, M. C.; Farkas, O.; Malick, D. K.; Rabuck, A. D.; Raghavachari, K.; Foresman, J. B.; Ortiz, J. V.; Cui, Q.; Baboul, A. G.; Clifford, S.; Cioslowski, J.; Stefanov, B. B.; Liu, G.; Liashenko, A.; Piskorz, P.; Komaromi, I.; Martin, R. L.; Fox, D. J.; Keith, T.; Al-Laham, M. A.; Peng, C. Y.; Nanayakkara, A.;

Challacombe, M.; Gill, P. M. W.; Johnson, B.; Chen, W.; Wong, M. W.; Gonzalez, C.; Pople, J. A. *GAUSSIAN 03* (Revision C.02), Gaussian, Inc.: Wallingford, CT, 2004.
(28) (a) Pasgreta, E.; Puchta, R.; Galle, M.; van Eikemma-Hommes, N.; Zahl, A.; van Eldik, R. *ChemPhysChem* **2007**, *8*, 1315−1320. (b) Pasgreta, E.; Puchta, R.; Zahl, A.; van Eldik, R. *Eur. J. Inorg. Chem.* **2007**, *13*, 1815−1822. (c) Schmidt, E.; Hourdakis, A.; Popov, A. I. *Inorg. Chim. Acta* **1981**, *52*, 91−95.
(29) (a) Ignatyev, N. V.; Welz-Biermann, U. *Chim. Oggi* **2004**, *22*, 42−43. (b) Yan, P.-F.; Yang, M.; Liu, X.-M.; Liu, Q.-S.; Tan, Z.-C.; Welz-Biermann, U. *J. Chem. Eng. Data* **2010**, *55*, 2444−2450.
(30) (a) Lassègues, J.; Grondin, T.; Talaga, D. *Phys. Chem. Chem. Phys.* **2006**, *8*, 5629−5632. (b) Umebayashi, Y.; Mitsugi, T.; Fukuda, S.; Fujimori, T.; Fujii, K.; Kanzaki, R.; Takeuchi, M.; Ishiguro, S. *J. Phys. Chem. B* **2007**, *111*, 13028−13032.
(31) Pokorny, K.; Schmeisser, M.; Troeppner, O.; Hampel, F.; Zahl, A.; Puchta, R.; van Eldik, R. In preparation.
(32) (a) Hofmeister, F. *Arch. Exp. Pathol. Pharmakol.* **1888**, *24*, 247−260. (b) Robinson, D. M. *Naturwissenschaften* **1978**, *65*, 438−439. (c) Thomas, A. S.; Elcock, A. H. *J. Am. Chem. Soc.* **2007**, *129*, 14887−14898. (d) Pegram, L. M.; Record, M. T., Jr. *J. Phys. Chem. B* **2007**, *111*, 5411−5417. (e) Leontidis, E.; Aroti, A. *J. Phys. Chem. B* **2009**, *113*, 1460−1467. (f) Pegram, L. M.; Wendorff, T.; Erdmann, R.; Shkel, I.; Bellissimo, D.; Felitsky, D. J.; Record, M. T., Jr. *Proc. Natl. Acad. Sci. U. S. A.* **2010**, *107*, 7716−7721.
(33) Schmeisser, M. Unpublished results.
(34) (a) Pasgreta, E.; Puchta, R.; Galle, M.; van Eikemma-Hommes, N.; Zahl, A.; van Eldik, R. *ChemPhysChem* **2007**, *8*, 1315−1320. (b) Pasgreta, E.; Puchta, R.; Zahl, A.; van Eldik, R. *Eur. J. Inorg. Chem.* **2007**, *13*, 1815−1822.
(35) (a) Wickleder, M. S. *Z. Anorg. Allg. Chem.* **2003**, *629*, 1466−1468. (b) Henderson, W. A.; Brooks, N. R. *Inorg. Chem.* **2003**, *42*, 4522−4524.
(36) Addison, A. W.; Rao, T. N.; Reedijk, J.; van Rijn, J.; Verschoor, G. C. *Dalton Trans.* **1984**, *7*, 1349−1356.
(37) (a) Illner, P.; Puchta, R.; Heinemann, F. W.; van Eldik, R. *Dalton Trans.* **2009**, *15*, 2795−2801. (b) Holbrey, J. D.; Reichert, W. M.; Rogers, R. D. *Dalton Trans.* **2004**, *15*, 2267−2271 and references cited therein.
(38) (a) Mudring, A. V.; Babai, A.; Arenz, S.; Giernoth, R. *Angew. Chem., Int. Ed.* **2005**, *44*, 5485−5488. (b) Mezailles, N.; Ricard, L.; Gagosz, F. *Org. Lett.* **2005**, *7*, 4133. (c) Babai, A.; Mudring, A. V. *Z. Anorg. Allg. Chem.* **2008**, *634*, 938−940. (d) Nockemann, P.; Thijs, B.; Lunstroot, K.; Parac-Vogt, T. N.; Görller-Walrand, C.; Binnemans, K.; Van Hecke, K.; Van Meervelt, L.; Nikitenko, S.; Daniels, J.; Hennig, C.; Van Deun, R. *Chem.—Eur. J.* **2009**, *15*, 1449−1461.
(39) Williams, D. B.; Stoll, M. E.; Scott, B. L.; Costa, D. A.; Oldham, W. J., Jr. *Chem. Commun.* **2005**, *11*, 1438−1440.